

Performance of HAWK-I: the new high acuity wide-field K-band imager

M.Kissler-Patig^a, N.Ageorges^b, C.Alves de Oliveira, L.R.Bedin^c, E.Bendek, M.Casali, R.Dorn, R.Esteves, G.Finger, D.Gojak, Y.Jung, M.Kiegebush, A.Moorwood, J.-L.Lizon, M.Petr-Gotzens, J.F.Pirard, J.Pritchard, F.Selman

^a All authors: European Southern Observatory (Garching/Germany and/or Vitacura/Chile);

^b currently: Max-Planck Institute für extraterrestrische Physik (Garching Germany);

^c currently: Space Telescope Science Institute (Baltimore/USA)

ABSTRACT

HAWK-I is the newly commissioned High Acuity Wide-field K-band Imager at the ESO Very Large Telescope. It is a 0.9–2.5 micron imager with a field of view of 7.5x7.5 arcmin sampled at 106 mas with four Hawaii2RG detectors. It has a full reflective design that was optimised for image quality and throughput. We present an overview of its performance as measured during the commissioning and first science runs. In particular, we describe a detector read-out mode that allows us to increase the useful dynamic range of the detector, and a distortion calibration resulting in <5mas relative astrometry across the field.

Keywords: Instrument, imager, near-infrared, ESO, VLT, HAWK-I

1. HAWK-I INSTRUMENT DESCRIPTION

HAWK-I is a cryogenic instrument now installed on the adapter/rotator of one of the Nasmyth foci of the VLT UT4. An overview of the HAWK-I characteristics is presented in Table 1.

Table 1. HAWK-I properties

Parameter	Value
Wavelength	0.9–2.5 microns
Plate scale	106 mas/pixel
Field of view	7.5 arcmin \times 7.5 arcmin
Image quality (80% EE)	<0.2 arcsec
Distortion	<0.3% across the field
Optics throughput (w/o detector)	>70%
Filters	4 Broad Band, 6 Narrow Band)
Detectors	four 2k \times 2k Hawaii2RG arrays
Detector Q.E.	> 80%
Detector Temperature	75 K \pm 1mK
Read noise	~ 5 e ⁻ for DIT>15 s
Instrument background	$\sim 0.10 - 0.15$ e ⁻ /s
Instrument Temperature	<140 K

With the exception of the entrance window, the optical design is based on an all reflective configuration. The purpose of the optical configuration is to adapt the F-number of the input beam to the pixel field-of-view requirement (0.1 arcsec /pixel) and to limit the stray light reaching the detector by means of a cold field stop located at the entrance of the instrument and the M3 mirror acting as a cold pupil stop.

Further author information: (Send correspondence to M.Kissler-Patig)
M.Kissler-Patig: E-mail: mkissler@eso.org, Telephone: +49-89-32006244

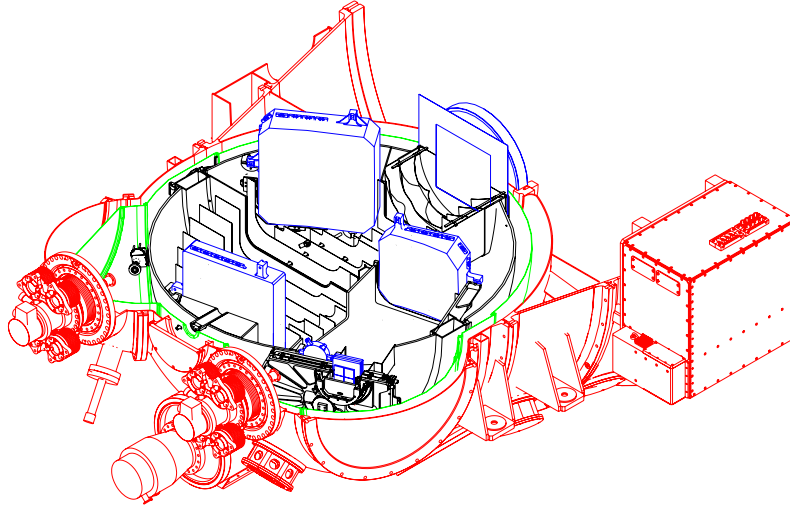


Figure 1. Cut through HAWK-I for an optical and mechanical overview. Blue: optical components; Black: cold assembly, filter wheels, detector assembly; Green: radiation shield; Red: Vessel structure, cryogenic components, electronic rack.

Just before the light reaches the detectors, two filter wheels allow the insertion of Broad Band (Y , J , H , K_s) and Narrow Band (interstellar lines and cosmological) filters.

The HAWK-I focal Plane is equipped with a mosaic of four $2K \times 2K$ Rockwell HgCdTe MBE HAWAII 2 RG arrays. The packaging of this 2×2 mosaic detector is provided by GL Scientific re-using the design developed for the JWST program. The acquisition system is based on the IRACE system (Infrared Array Control Electronics) developed at ESO.

The optics and focal plane are mounted on a spherical cold structure which provides the mechanical stability between the different elements. This assembly is cooled to cryogenic temperature using a liquid nitrogen pre-cooling circuit and two closed cycle coolers. The detectors and the filter wheel unit are connected to the second stage of the Closed Cycle Cooler and operated at a temperature close to 75-80 K. A temperature below 140 K is achieved for the rest of the instrument.

The vacuum vessel containing the instrument is interfaced to the Nasmyth adaptor. The interface flange is designed such that it can accommodate the further installation of wavefront sensors required for the operation with a later adaptive secondary mirror of the telescope.

The specification of the camera was largely driven by the four $2k \times 2k$ $0.9\text{-}2.5\mu\text{m}$ Rockwell array detectors, i.e. the facts that *i*) four was the largest number of arrays we could mosaic and *ii*) we wished to be seeing limited under the best conditions on Paranal. We thus specified 0.106 arcsec pixels (cf. ISAAC 0.147 arcsec) which yields a field of $7.5 \text{ arcmin} \times 7.5 \text{ arcmin}$. Moreover, this pixel sampling of 0.106 arcsec is fully compatible with the expected wide field image quality improvement provided by the Adaptive Secondary mirror (to come around 2012) without any loss of resolution.

HAWK-I is also designed to work in the future with a ground-layer adaptive optics module (GRAAL) as part of the Adaptive Optics Facility [1] for the VLT. The facility is expected at the telescope around 2012, at which point the GRAAL module will be brought into operation. This module is inserted between the telescope adapter/rotator and the HAWK-I entrance window and is equipped to sense the wave-front of four laser guide stars and one natural guide star and to feed back corrections to the adaptive secondary mirror of the VLT. The module aims at correcting the ground-layer turbulence over the complete field-of-view, i.e. not at achieving diffraction limited images but rather at improving significantly the seeing/image quality of the near-infrared images.

2. HAWK-I PERFORMANCE

This section summarises the main characteristics of HAWK-I and its performance as measured during commissioning. More details and updates are available through the instrument web pages at ESO (www.eso.org/instruments/hawki).

2.1 Detector characteristics and field-of-view

2.1.1 Field-of-view coverage

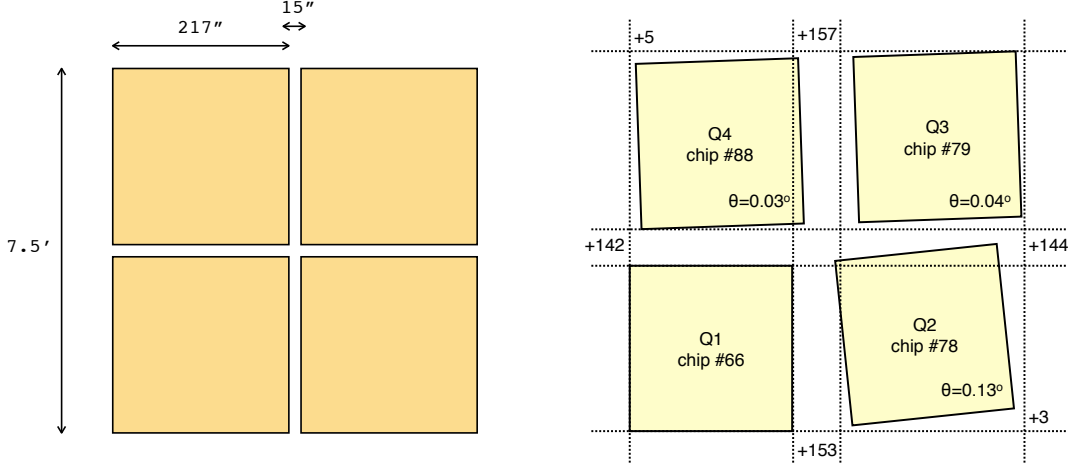


Figure 2. HAWK-I field-of-view coverage by the detector mosaic. *Left*: The layout of the field of view on the sky - note the small gap of ~ 15 arcsec between the four detectors. *Right*: The relative orientation of the four detectors with the average gap size given in pixels.

The $7.5 \text{ arcmin} \times 7.5 \text{ arcmin}$ field-of-view of HAWK-I is covered by four Hawaii-2RG chips of 2048^2 pixels each (1 pixel corresponds to 0.106 arcsec on the sky). The detectors are separated by gaps of about 15 arcsec as shown in Fig. 2. The figure also shows the naming convention of the four detectors. The images of the four detectors are stored together in a single FITS file as four extensions. Note that quadrants 1,2,3,4 are usually, *but not necessarily*, stored in extensions 1,2,4,3 of the HAWK-I FITS file *.

Table 2. HAWK-I field-of-view vignetting

Edge	No of columns or or rows vignettted $> 10\%$	Maximum vignetting ^a
+Y	1	14%
-Y	8	54%
-X	7	36%
+X	2	15%

^aThe last column represents the maximum extinction of a vignettted pixel, i.e. the percentage of light absorbed in the pixel row or column, with respect to the mean of the field.

Finally, due to necessary baffling in the all-reflective optical design of HAWK-I, some vignetting at the edges of the field has turned out to be inevitable due to positioning tolerances of the light baffles. The vignetting measured on sky is summarised in Table 2. Note that although the +Y edge vignetting is small in amplitude, it extends to around 40 pixels at $< 10\%$.

*Re-naming the quadrants would have caused confusion in the design documentation; re-ordering the quadrants in the detector electronics would generated read-out overhead; and last but not least, the FITS convention forbids to identify extensions by their location in the file. For unambiguous identification, the FITS keyword EXTNAME in each extension should be used (eg. EXTNAME = CHIP1.INT1, referring to Q1 or chip#66).

2.1.2 Detector characteristics

The characteristics of the four detectors are summarised in Table 3. Note that for detector integration times (DIT) greater than 15s the read-out noise (RON) of the detector is as low as $\sim 5 e^-$. The Hawaii2RG detectors have four reference columns/rows around each device which are not sensitive to light.

Table 3. HAWK-I detector characteristics

Detector Parameter	Q1	Q2	Q3	Q4
Detector numbering	#66	#78	#79	#88
Operating Temperature	75K, controlled to 1mK			
Gain [e^- /ADU]	1.705	1.870	1.735	2.110
Dark current (at 75 K)	$< 0.01 e^-$ /s/pix			
Read-out noise (NDR) ^a	~ 5 to $12 e^-$			
Linear range (1%)	$60.000 e^-$ (~ 30.000 ADUs)			
Saturation level	between 40.000 and 50.000 ADUs			

^aThe read-out noise (RON) in the default Non-Destructive Read (NDR) mode depends on the DIT: the detector is read continuously every ~ 1.3 s, i.e. the longer the DIT, the more reads are possible and the lower the RON. For the minimum DIT (1.3s), the RON is $\sim 12 e^-$; for DIT=10s, the RON is $\sim 8 e^-$ and for DIT>15s, the RON remains stable at $\sim 5 e^-$.

2.1.3 Threshold Limited Integration

The HAWK-I detector is operated by default in a non-destructive read-out mode (see above). For HAWK-I, we have implemented a variation of this mode: the Threshold Limited Integration (TLI), see Fig. 3.

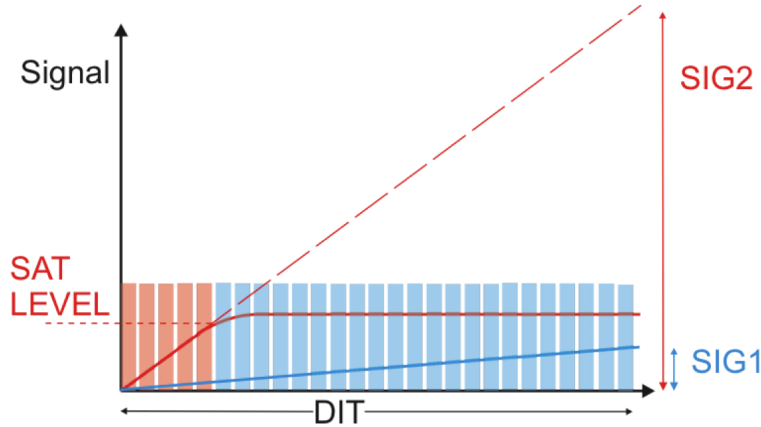


Figure 3. HAWK-I's Threshold Limited Integration mode. Only pixel values below SATLEVEL are taken into account for calculation of slope for pixels with high flux (red line). For low flux pixels (blue line) all non-destructive readouts indicated by rectangles are used. The final FITS file contains the values SIG1 and SIG2, allowing to exceed the saturation level of the detector.

For a non-destructive read-out, it is possible to define a threshold (e.g. a value below the saturation limit) above which the read-out values are not taken into account anymore. I.e. for a bright star reaching the saturation limit during the detector integration time (DIT), only the values read before the star goes into saturation are taken into account (see red line in Fig. 3), and the pixel value written into the FITS file is the value extrapolated to the full integration time (calculated from the slope of the non-saturated, non-destructive read-outs). All pixels which have absolute ADU values below this threshold over the integration time (DIT) are processed normally (blue pixel in Fig. 3).

The great advantage is of course that most bright objects do not saturate in the final FITS file and that (depending on the DIT) the dynamic range is increased (by typically 2 mag for a 30s DIT). The pixels may be physically saturated of

course, i.e. the persistence (which is important for highly saturated pixels in HAWK-I) remains. Another caveat is that the *effective* integration time for bright stars is not the DIT, but the time until the star reached the saturation limit - which will alter the noise properties for bright stars - although not critically as the S/N is high. Finally, a very bright star (of the order of < 9 mag) will saturate within the first non-destructive read and will not profit from the TLI mode.

Tests have verified that the photometry is not altered at a detectable level for stars above the threshold. Yet, it is recommended that for precise photometry ($< 5\%$) only stars below the threshold (typically set to 30.000 ADU) be used.

A user that does not want to make use of this mode, can simply flag all pixels above the value recorded in the header keyword DET.SATLEVEL (typically 30.000) to NaN.

2.2 Filter system

HAWK-I hosts two filter wheels of six position each. Each wheel has an open position, leaving room for two times five filters: 4 broad band filters, and 6 narrow band filters.

Table 4. HAWK-I filter summary

Filter name	central wavelength [nm]	cut-on (50%) [nm]	cut-off (50%) [nm]	width [nm]	transmission [%]	comments
Y	1021	970	1071	101	92%	out-of-band transmission of 2×10^{-4} (or 0.04%) between 2.3 and $2.7 \mu\text{m}$
J	1258	1181	1335	154	88%	
H	1620	1476	1765	289	95%	
K_s	2146	1984	2308	324	82%	
CH_4	1575	1519	1631	112	90%	
$\text{Br}\gamma$	2165	2150	2181	30	77%	
H_2	2124	2109	2139	30	80%	
NB1060	1061	1057	1066	9	70%	$\text{Ly}\alpha$ at $z \sim 7.7$
NB1190	1186	1180	1192	12	75%	$\text{Ly}\alpha$ at $z \sim 8.7$
NB2090	2095	2085	2105	20	81%	$\text{H}\alpha$ at $z \sim 2.2$

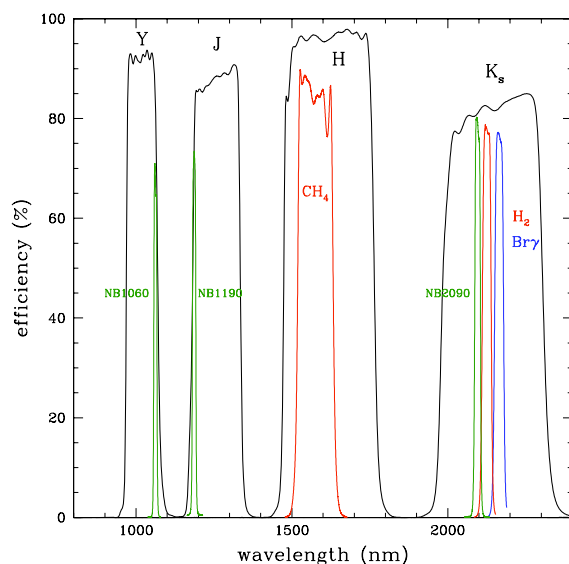


Figure 4. HAWK-I filter transmission curves

The broad-band filters Y , J , H , K were ordered following the Mauna Kea Observatory specifications (see [10], [9]). This standardization allows an easy cross-calibration and comparison between HAWK-I and the UKIDSS survey [6] as well as the VISTA infrared camera [4].

The narrow band filters include three cosmological filters for $\text{Ly}\alpha$ at $z \sim 7.7$ (at $1.06 \mu\text{m}$) and $z \sim 8.7$ (at $1.19 \mu\text{m}$), and $\text{H}\alpha$ at $z \sim 2.2$ (at $2.09 \mu\text{m}$) as well as three ‘galactic’ filters (CH4 , H_2 , $\text{Br}\gamma$). The filter properties are summarised in Table 4, and the filter transmission curves are shown in Fig. 4. The transmission curves are available in electronic form on the instrument web pages (www.eso.org/instruments/hawki/).

2.3 Photometric performance

2.3.1 Limiting magnitude

HAWK-I is a highly effective imager with a total instrument throughput, including detectors, close to 60% in the Y , J , H bands, and over 50% in the K band.

The limiting magnitudes are of course very much dependent on the observing conditions. The exposure time calculator, available through the ESO web pages (www.eso.org/observing/etc/), is well calibrated and can be used to estimate the performance in all filters.

As an example, we give in Table 5 the limiting magnitudes ($S/N=5$ for a point source in 3600s integration on source) and saturation limits for broad band filters in average conditions (0.8 arcsec seeing, 1.2 airmass).

Table 5. HAWK-I limiting magnitudes and saturation limits ($S/N=5$ for 1h on source, 0.8 arcsec seeing, 1.2 airmass)

Filter	Limiting mag [Vega]	Limiting mag [AB]	Saturation limit (in 2 sec)
J	23.9	24.8	11.0
H	22.5	23.9	11.3
K_s	22.3	24.2	10.2

2.3.2 Calibrating photometry with HAWK-I, using the 2MASS catalogue

A calibration plan assures that the performance is monitored every night and has shown that HAWK-I is extremely stable.

Calibration of the photometry to $\sim 5\%$ across the field, can be achieved in two ways. Photometric standard stars from the standard catalogues (UKIRT faint standards, [5]; Persson list of standards, [8]) can be measured before/between/after the observations, moving the standard stars through all four quadrants.

Alternatively, the numerous 2MASS calibrated stars present in the frame can be used to derive the zero points. Indeed, the HAWK-I field of view is large enough to usually include 10 to 100 calibrated 2MASS stars. Each star cannot be measured with the precision of a photometric standard star, but is typically catalogued with photometry good to <0.1 mag. The large number across the field permits the determination of the zero point on the image to ~ 0.05 mag, using these local secondary standards. Extinction coefficients are then automatically taken into account and the colour terms for HAWK-I can also be derived.

The above determination of the zero points and colour terms should be performed after the illumination correction. For this purpose, an illumination map is built by observing stars in a grid on each detector. Zero points are derived as a function of position on the chip and a map is interpolated. The variations of the zero point are typically smaller than a few percent in the broad band filters.

2.4 Astrometric performance

For a full analysis of the astrometric performance of HAWK-I, we refer to [3]. Here we draw attention to a few points to note when translating detector coordinates into relative or absolute coordinates on the sky.

2.4.1 Centre of rotation and centre of pointing

The optical axis of the telescope is not perfectly aligned with the one defined by the center of the detector mosaic. The difference being small, this is not physically corrected for by the telescope control software. In the standard orientation (North is +Y, East is -X) the centre of the detector array is located ~ 0.4 arcsec East and ~ 0.4 arcsec South of the telescope pointing, i.e. shifted by 4 pixel on each axis.

The world coordinate system (WCS) provided in the header of each quadrant takes this into account, however. Further, the WCS of each quadrant is defined such that it refers (c.f. CRPIX keywords) to the reference pixel taken to be the central pointing (and centre of rotation) of the telescope (i.e. the TEL.TARG.RA and TEL.TARG.DEC keywords reported in the header).

2.4.2 Distortion correction

The optical distortions across the HAWK-I field of view are very small (0.1% at the worst). They were measured following the auto-calibration method of [2] and we refer to [3] for the full details. The worst variation of the non-linear part of the distortions from the center of the detector is ~ 2.9 pixels, for a diagonal of a quadrant of ~ 2900 pixels.

A distortion map (shown in Fig. 5) is produced regularly in the form of a look-up table of corrections to be applied to the x and y coordinates (as a function of position in the field) in order to recover the undistorted position. The correction is given for coordinates defined in an (arbitrarily chosen but now fixed) meta-frame coordinate system.

Currently, the best distortion map allows a recovery of relative positions with an rms of < 5 mas across the entire field.

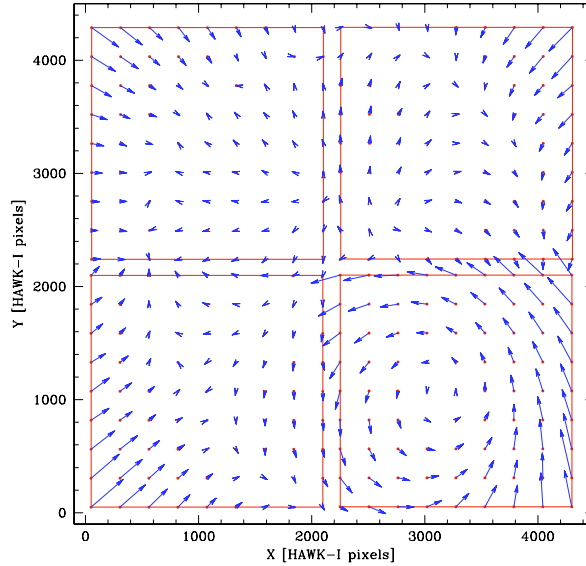


Figure 5. HAWK-I distortion map. The red boxes show the positions of the single HAWK-I chips in the meta-chip system. The red dots are our grid points in the look-up table used to represent the geometrical distortion. The arrows give the sizes (exaggerated by a factor 100) and the directions of the correction to be applied to the grid-points to bring them into a distortion free frame. The correction for any pixels in the detector can be obtained with a bi-linear interpolation of the 4 closest grid-points.

2.4.3 Image quality

The image quality over the HAWK-I field is very homogeneous.

We evaluated the image quality on images taken in very good seeing conditions: down to an average image quality of ~ 0.25 arcsec FWHM across the field, no trend in systematic elongation or preferred orientation of the PSF is detectable.

Only for a combined image with an average image quality of ~ 0.23 arcsec did we observe a ~ 0.1 arcsec (i.e. 5%) degradation of the image quality towards the edges of the $7.5 \text{ arcmin} \times 7.5 \text{ arcmin}$ field that could be attributed to the HAWK-I optics.

We conclude that for most observation, the user will not notice significant changes of the PSF across the entire field.

3. CONCLUSIONS

The HAWK-I field-of-view and plate scale, combined with the very high throughput and outstanding image quality make this instrument the most performant near-infrared imager on an 8m-class telescope to date.

First scientific results were obtained during science verification and are available worldwide through the ESO archive.

REFERENCES

- [1] Arsenault et al. 2006, *The Messenger*, 123, 6
- [2] Anderson, J., Bedin, L.R., Piotto, G., Yadav, R.S., Bellini, A. 2006, *A&A* 454, 1029
- [3] Anderson, J., Bedin, L.R., et al. in preparation
- [4] Dalton, G.B., Caldwell, M., Ward, A.K. et al. 2006, *SPIE* 6269, 30
- [5] Hawarden, T.G., Leggett, S.K., Letawsky, M.B., Ballantyne, D.R., Casali, M.M. 2001, *MNRAS* 325, 563
- [6] Hewett, P. C., Warren, S. J., Leggett, S. K., Hodgkin, S. T. 2006, *MNRAS* 367, 454
- [7] Jung, Y. et al.: *The HAWK-I Pipeline User Manual (VLT-MAN-ESO-19500-4407)*, 2008, ESO
- [8] Persson, S.E., Murphy, D.C., Krzeminski, W., Roth, M., Rieke, M.J. 1998 *AJ* 116, 2475
- [9] Simons, D.A. & Tokunaga, A.T. 2002, *PASP* 114, 169
- [10] Tokunaga, A.T. & Vacca, W.D. 2005, *PASP* 117, 421